

Two Photon Microscopy and Second Harmonic Generation

Leif Gibb and David Matthews

Introduction and Background

Nonlinear microscopy has become an important tool for imaging biological samples such as neurons. In two photon fluorescence, a fluorophore absorbs two photons at a low energy state, one of its electrons briefly converts to a higher energy state, and it emits a single excited photon at an energy level higher than that of the absorbed photons. In second harmonic generation (SHG), laser light is focused on a sample to generate frequency-doubled light: two photons of one wavelength are annihilated and a single photon of half the wavelength is generated.

As neurobiology increasingly addresses the cellular and circuit-level underpinnings of behavioral and systems-level phenomena, pushing nonlinear microscope technology to diffraction-limited spatial and unlimited temporal extents is necessary. The development of novel nonlinear techniques has revealed much in the last decade and a half of neuroscience, and promises the possibility of a much richer functional understanding of the brain. In light of the importance of this technique, we were interested in using a prefabricated laser to build a two photon and SHG microscope. Thus, in the present work, we had several goals: 1) to generate 2-photon fluorescence from a cuvette of Rhodamine dye; 2) to create labeled lipid membranes on planar glass supports for use in SHG; 3) to achieve 2-photon fluorescence and SHG from labeled lipid membranes; 4) to demonstrate SHG from a nonlinear crystal.

Two Photon Microscopy and Fluorescence

Two photon laser microscopy (TPLM) is a technique in which photons of a pulsed laser collide in a femtoliter-order volume of sample. It is especially useful to biology because of its selective excitation, the theory of which came in 1931 from Maria Göppert-Mayer. She recognized that a fluorophore could simultaneously absorb two photons at a low energy state and emit one photon at a higher energy state. The technology was gradually developed: in 1960 Ted Maiman built the first working laser, by 1982, two photon microscopy was used for spectroscopic examination of molecular excitation states (Friedrich, 1982), and within a decade, Winfried Denk and Watt Webb had developed the two-photon laser for application to neurobiology (Denk et al., 1990).

A laser is a coherent beam of intense light generated by energizing one or a set of ions from a ground- to a metastable- molecular state. Traditional laser methods achieve this state change by a population inversion, in which intense radiation at room temperature moves the majority of ions from the ground to the excited state. Their inevitable relaxation—at thermal equilibrium—from this excited state back to ground state releases photons in a beam by a process called stimulated emission (Hecht, 2002).

When photons coherently leave the laser encasement, they have sufficient energy to excite certain fluorophores in a sample. In traditional fluorescence microscopy, if the

emission wavelength of the laser and the absorption spectrum of the fluorophores align, excitation occurs. In two photon fluorescence, the simultaneous absorption of two photons of half the frequency of the absorption spectrum of the fluorophore is required for fluorescence. The likelihood of simultaneous absorption of two photons in natural light is small: a back of the envelope calculation suggests that sunlight might cause 1 event/ 10^6 years (Webb, 1997). Therefore, fluorescence using TPLM involves a mode-locked laser, in which photons are emitted at a frequency of order femtoseconds⁻¹ or greater. That is, the intensity of light emitted is high for short bursts of time. Because the likelihood of simultaneous absorption events increases supralinearly with the population of photons emitted, just as a Hill coefficient of $n = 2$ in physical chemistry, this greater intensity leads to many more absorption events. For example, mode-locking in a Ti:Sapphire laser increases the probability of absorption by 10^5 relative to a continuous wave with the same average power (Webb, 1997).

Mode-locking and two photon absorption render TPLM advantageous over its predecessors for many applications. In particular, with such a small focal volume in which fluorophores are excited, there is little wasted fluorescence: the fluorescence emission of all excited molecules is captured and imaged at once. This is in stark contrast to confocal microscopy, in which a pinhole blocks all but a small section of the fluorescence from a section of a sample while intense laser light excites fluorophores throughout the entire sample. Many problems that come with confocal microscopy—fast fluorescence decay with time, increased light scattering, wasted fluorescence excitation, increased photodamage, and increasingly poor resolution with depth in the sample—are therefore avoided with the mode-locked, slower wavelength laser light of TPLM.

Nonlinear Optics and Second Harmonic Generation

Although a complete review of nonlinear optics is beyond the purview of this paper, what follows is a brief discussion as a primer for our experiments with second harmonic generation.

Nonlinear optics is concerned with phenomena resulting from light-induced changes to the optical properties of a system. Such phenomena are ‘nonlinear’ in that they depend quadratically on the strength of the optical field. Second harmonic generation is an appropriate example of such nonlinearity: the intensity of the light resulting from second harmonic generation scales with the square of the applied laser light.

The following is an informal mathematical description of second harmonic generation, starting with an intuitive description of nonlinear optics.

The polarization $P(t)$, the dipole moment per volume, of a system depends on the strength $\hat{E}(t)$ of the optical field. In conventional optics, this relationship is linear:

$$P(t) = \chi^{(1)} \hat{E}(t)$$

where the constant $\chi^{(1)}$ is called the linear susceptibility. However, in nonlinear optics, the generalization of this equation attains, in which the polarization goes with the power series of the field strength:

$$\begin{aligned} P(t) &= \chi^{(1)} E(t) + \chi^{(2)} E^2(t) + \dots + \chi^{(n)} E^n(t), \\ P(t) &= P^{(1)}(t) + P^{(2)}(t) + \dots + P^{(n)}(t) \end{aligned}$$

where $\chi^{(n)}$ is the nth-order nonlinear optical susceptibility and $P^{(n)}(t)$ is called the nth-order polarization. When a laser with an electric field strength given by

$$\hat{E}(t) = Ee^{-i\omega t} + \text{complex conjugates}$$

impinges on a system with a nonzero second-order susceptibility $\chi^{(2)}$, the polarization created is

$$P^{(2)}(t) = 2\chi^{(2)} EE^* + \chi^{(2)} E^2 e^{-2i\omega t} + \text{complex conjugates}.$$

Clearly, this second-order polarization has a zero frequency component, in which $\omega = 0$, and a frequency 2ω component, accurately accounting for the empirical observation of second harmonic generation (Boyd, 1992, pp. 1-5, 17-21, and 78-84).

A pictorial representation of the second harmonic generation phenomenon is shown in Fig. A1. The first image is a block diagram noting the input to and output from the nonlinear optical material. The second image is an energy-level diagram of the phenomenon.

SHG light is emitted coherently (Millard et al. 2001). It occurs at noncentrosymmetric loci (that is, loci lacking a center of symmetry; Moreaux et al. 2001). In biological samples, noncentrosymmetric loci can be found, for example, at cellular membranes in which the outer leaflet is labeled by a dye (Moreaux et al. 2001), at myosin filaments (Both et al. 2004), in collagen (Williams et al. 2005) and in cellulose (Brown et al. 2003). SHG has emerged as a technique for optical recording of membrane potential in dye-labeled membranes (Bouevitch et al. 1993, Millard et al. 2003, Nemet et al. 2004, Campagnola et al. 2002); for example, this technique has recently been used to image membrane potential in dendritic spines (Nuriya et al. 2005) and in cultured *Aplysia* neurons (Sacconi et al. 2006). Because SHG is coherent and sensitive to phase, it can provide information about molecular spatial organization in a manner that fluorescence does not. For example, when two labeled giant unilamellar vesicles (GUVs) undergo adhesion, so that their membranes are closely apposed, dye molecules at the adhesion zone are centrosymmetrically arranged, and destructive interference of the SHG light occurs (Moreaux et al. 2001). Destructive or constructive interference of SHG light may occur depending on the distance between GUV membranes.

Methods and Results

Optical apparatus

Our basic optical apparatus (Tsai et al, 2002) is shown in Fig. 1. Laser light was reflected off of a mirror, and ~8% of the light was reflected by a microscope slide for detection by a photodiode. Detection at this point was used to verify mode locking of the laser (see Appendix 1 for further description of the laser). The laser light along the main beam path was then reflected off of another mirror, passed through a beam expander consisting of a confocal pair of lenses (25.4 mm and 160 mm focal lengths). This expanded the beam 6-fold so that it filled the back of an objective, which focused the light onto the sample. Light from the sample was then collected in one of three ways: 1) by a single collector lens placed $2f$ from the sample and $2f$ from a photodiode; 2) by a pair of lenses, one $1f$ from the sample and the other $1f$ from a photodiode. 3) By a spherical lens placed close to the sample, again focusing light onto a photodiode; 4) By a cooled CCD camera focused on the sample. For cases 1-3, the photodiode was connected to an oscilloscope to observe its voltage responses. For case 4, the CCD camera was connected to a monitor for observation.

Optical filters

We had three different filter types to help verify SHG and fluorescence: 1. A set of four blue-green filters, passing a broad set of wavelengths below about 600 nm (i.e. both SHG and light emitted fluorescently from a dye like Rhodamine 6G). 2. A filter (“SHG filter”) passing a narrow set of wavelengths between 500 and 540 nm (around the expected wavelength of SHG light, 515 nm), and also a broader set of wavelengths above 725 nm. 3. A high-pass filter passing light above about 550 nm but blocking longer-wavelength light. They were placed between the objective or the CCD and the sample itself.

The fluorescence emission spectra of Rhodamine 6G, Rhodamine B, diI, di-4-ANEPPS, and di-8-ANEPPS are shown in Fig. 3. All peak between 550 and 650 nm. We expect the blue-green filters to pass fluorescence from Rhodamine 6G, Rhodamine B, and diI, and to pass some (but less) fluorescence from the ANEPPS dyes. They will also pass SHG light. Thus, a large signal detected with the blue-green filters in place must be fluorescence and/or SHG light. For diI, di-4-ANEPPS, and di-8-ANEPPS, a large signal detected with the blue-green filters plus the SHG filter in place must be SHG light. Additionally, the high-pass filter should block the SHG light.

Generation of two photon fluorescence from Rhodamine dye

The goal of this portion of our work was to generate and detect two photon fluorescence from a cuvette of Rhodamine dye.

We mounted a flat cuvette of Rhodamine 6G near the objective focus, and then finely adjusted the distance to the objective until we observed a small point of reddish light in the cuvette, suggesting two photon fluorescence at the objective focus. However, we found that the blue-green filters (one or more) completely blocked the oscilloscope signal from the photodiode, implying that the photodiode was not detecting fluorescence within the wavelengths passed by these filters, i.e. below about 600 nm. However, we note that the reddish light would obviously be expected to be above 600 nm. This result was observed with all lens configurations described above.

We also tried the same experiment with a cuvette of Rhodamine B. In this case, we did not observe fluorescence, even by eye.

Creation of lipid membranes

The goal of this portion of our work was to create dye-labeled lipid membranes with the appropriate characteristics for SHG.

Our early efforts used asolectin provided by M. Montal, a mixture of soybean lipids containing ~30% phosphatidylcholine, ~30% phosphatidylethanolamine, ~8% cardiolipin and other neutral lipids (M. Montal, personal communication). Our later, more successful, efforts used 1,2-dioleoyl-*sn*-glycero-3-phosphocholine (DOPC, Avanti Polar Lipids). This lipid has been used by Moreaux et al. (2000; Sandre et al. 1999) to create giant unilamellar vesicles for their SHG experiments. However, it should be possible to create lipid membranes with either of these lipid sources. The fact that the DOPC was already dissolved in chloroform enabled us to avoid the initial step of dissolving the asolectin in an organic solvent.

We considered a number of alternative methods for creating labeled lipid bilayers. Moreaux et al. (2001) have studied SHG from GUVs labeled on their outer leaflet. SHG is generated by dye molecules restricted to the outer leaflet; the inner leaflet is not labeled. GUVs can be created either by extrusion (White et al. 1996; <http://www.avantilipids.com/LUVET.html>) or by creating small unilamellar vesicles (SUVs) and keeping them below the phase transition temperature of the lipid for several days or weeks to promote spontaneous fusion (Wong et al. 1982; Lichtenberg et al. 1986).

A second method is based on work by Montal and Mueller (1972). In this method, a hydrophobic film with a small aperture is lowered between two troughs containing lipid monolayers on the surface of water. The hydrophobic chains tend to contact the hydrophobic surface, facilitating the formation of a bilayer at the aperture. Like the formation of GUVs, this method permits the formation of a bilayer with only one labeled leaflet. However, it requires a relatively complex setup and results in a bilayer that is, inconveniently, restricted to a small aperture.

A third method uses a monolayer deposited on a hydrophobic surface. This is accomplished by dipping the hydrophobic material into water that has a monolayer on its

surface, as in the technique of Montal and Mueller (1972; http://www.inapg.inra.fr/ens_rech/siab/asteq/elba/x-depos.htm) described above. The monolayer is labeled with a dye, and the requirement for noncentrosymmetry is met at the lipid-substrate interface. To our knowledge, this method has not been used previously in investigations of SHG. It is not clear if additional steps to mechanically compress the monolayer on the water surface (as in the Langmuir Blodgett technique; http://www.inapg.inra.fr/ens_rech/siab/asteq/elba/lb_tech.htm) are necessary.

A fourth method uses a monolayer deposited on a hydrophilic surface (hydrophobic tails pointing outwards; http://www.inapg.inra.fr/ens_rech/siab/asteq/elba/y-depos.htm). We attempted to generate a monolayer on the surface of a phosphate buffer solution by dropping the lipid-chloroform solution on the surface of the aqueous solution and letting the chloroform evaporate (Stottrup et al. 2004, http://www.inapg.inra.fr/ens_rech/siab/asteq/elba/y-depos.htm). However, the drops tended to join together into larger drops and/or sink. In some cases, we agitated the solution, which created a mixture containing smaller lipid aggregates. To this mixture we added DiI, which visibly labeled the lipid. We then dipped glass coverslips in the mixture. The coverslips picked up varying amounts of the lipid aggregates. It seems unlikely that the lipid was deposited as a monolayer, given its rather granular appearance.

We chose our current method on the basis of simplicity and likelihood of success. It involves the formation of a lipid bilayer on a planar glass support (Brian and McConnell 1984, Sackmann 1996, Cremer and Boxer 1999, Schonherr et al. 2004). In our current protocol, we prepared a buffer solution of 10 mM HEPES, 10 mM KCl, and 10 mM CaCl₂ (a subset of the solutes described in Brzezinski et al. 1998). In some cases, we omitted the CaCl₂. We evaporated chloroform from 1 mL of the 20 mg/mL lipid solution in a shallow dish in a fume hood, then hydrated the lipid in 2 mL of the buffer solution, to create a 10 mg/mL lipid suspension. To create small unilamellar vesicles (SUVs) we sonicated the lipid suspension for 40-60 min., with the heat on for approximately 20 min (<http://www.avantilipids.com/PreparationOfLiposomes.html>). We briefly dipped a glass coverslip in a shallow dish of the SUV suspension several times. The lipid was deposited on a portion of the side of the coverslip that faced down in the suspension. It is not clear whether the lipid was deposited as a bilayer or not, nor if so, how continuous the bilayer was. The coverslip was then set to dry on its other side. After drying, one of three dyes was added: Di-4-ANEPPS, Di-8-ANEPPS (both dissolved in dissolved in 95% ethanol), or 1,1'-Dioctadecyl 3,3,3',3'-Tetramethylindocarbocyanine Perchlorate (DiI; dissolved in 95% ethanol). Di-4-ANEPPS, Di-8-ANEPPS are voltage-sensitive dyes that bind and remain localized to the outer leaflet of cellular membranes; it is conceivable that they might also become restricted to the outer leaflet of supported lipid bilayers when applied on the outer bilayer surface. In cells, Di-8-ANEPPS is better retained in the outer membrane than Di-4-ANEPPS (<http://probes.invitrogen.com/handbook/sections/2202.html>). We observed the dye spreading several mm or more across the lipid deposited on the glass surface.

Previously, we tried a number of other methods. In one method, we prepared the DOPC by evaporating chloroform with a stream of nitrogen. We hydrated the lipid with a

volume of phosphate buffer roughly equal to the volume of evaporated chloroform, to create a roughly 20 mg/mL lipid suspension. We then sonicated the lipid suspension to create SUVs. After sonication, we added a small amount of diI.

Two photon fluorescence and SHG from a lipid sample

The goal of this portion of our work was to generate and detect two photon fluorescence from a lipid sample created by one of the above methods.

We observed a small point of reddish light in one of our more thickly deposited diI-labeled lipid samples, created by the *fourth method* described above. Again, the blue-green filters (one or more) completely blocked the signal, indicating that the photodiode was not detecting fluorescence (or SHG) within the wavelengths passed by these filters. Again we note that the reddish light would be expected to be above 600 nm.

SHG from a nonlinear crystal

In our final experiment, we used a single lens to focus laser light onto a nonlinear crystal, obviating the need for the beam expander lenses or the objective. In theory, the laser should be polarized with a polarization lens, impinge on the SHG crystal at the correct polarization, pass through the combination of SHG filter and blue-green filters, and be blocked by the high-pass filter. We attempted to detect this light with a cooled CCD camera connected to a video monitor. We expected a unique spatial pattern of SHG light to appear. In particular, we anticipated seeing a tight circle of SHG light surrounded by a remnant of emitted light, because the n-harmonic generated light goes with \sqrt{n} . We were unable to detect SHG light at any angle of rotation of the polarization lens. Most of the light was blocked by the blue-green filters, and we did not see the expected spatial pattern. We then re-tested the laser for mode-locking and found that it had (again) lost mode-locking, and was thus unsuitable for this experiment.

Discussion

To summarize, our results so far are the following: 1. We have seen evidence of two photon fluorescence from Rhodamine 6G and one of our diI-labeled lipid membrane samples by eye, but we have so far been unable to detect this fluorescence with a photodiode. 2. We have successfully deposited labeled lipids on glass supports. 3. We have not yet seen evidence for SHG generation from labeled lipid membranes. 4. Technical problems beyond our control (loss of mode-locking in the laser) prevented us from demonstrating SHG from a nonlinear crystal.

Five elements must work in tandem to achieve our goals. 1) The laser must be mode-locked. 2) The optics must be correct and appropriately optimized. 3) The detection instrumentation must be sufficiently sensitive. 4) The filters must pass appropriate wavelengths. 5) For SHG, the labeled lipids must contain noncentrosymmetric loci (such as those found when the outer leaflet of a bilayer is labeled). So far, we believe we have achieved two to four of these criteria at a time but not all five simultaneously.

The next steps we need to take are: 1) reestablish mode locking in the laser, or obtain a new mode-locked laser; 2) obtain SHG with a nonlinear crystal; and 3) generate and detect fluorescence from Rhodamine sample.

There are a number of ways that our experimental protocol could potentially be improved. For example, the power at the focus (and thus the fluorescence and SHG) could probably be increased by expanding the beam to a lesser degree, e.g. 4x instead of 6x. It would also be useful to have low-pass filters with a higher cutoff than the blue-green ones, to pass more of the fluorescence at higher wavelengths. However, given the fluorescence emission spectra of Rhodamine 6G and diI, they should generate a large amount of fluorescence below 600 nm (it is not clear that the fluorescence should be reddish).

We suspect that the lack of sensitivity of our photodiode has been an obstacle to detecting and recording fluorescence from a cuvette of Rhodamine dye, SHG from labeled lipid membranes, and SHG from a nonlinear crystal. It should be possible to obtain these data by using either a photomultiplier tube or a CCD camera. Only the lack of mode-locking in our later experiments prevented us from verifying this with a CCD camera.

With regard to lipid bilayer formation, published reports indicate that coverslips are typically prepared by washing in detergent, rinsing, and baking in a kiln (Brian and McConnell 1984, Cremer and Boxer 1999, Schonherr et al. 2004). One method uses centrifugation of the SUV suspensions after sonication to separate larger lipid structures from the SUVs (Cremer and Boxer 1999). This could improve the uniformity of deposition on the cover slip. Additionally, after bilayer formation, excess vesicles were washed away. It is likely that our results could be improved by following one of these published protocols in finer detail.

However, given the possibility that this technique will not enable us to confine dye molecules to just one leaflet, it would be sensible to try an approach that has been shown to result in SHG, namely creation of GUVs and labeling of the outer leaflet (Moreaux et al. 2001). The technique used by these researchers to create GUVs is described by Sandre et al. (1999).

Another future direction will be to further emulate the work of Moreaux et al. (2001) by developing a laser scanning system to fully image the GUVs.

Appendix 1: Laser

We used a mode-locked Magellan Yb-doped fiber laser oscillator (Clark-MXR, Inc) with a wavelength of 1030 nm, a pulse width < 200 fs, a nominal repetition rate of 37 MHz, and ~40 mW average power.

To verify that the laser was mode locked, we used a photodiode to detect laser light reflected from a glass microscope slide oriented ~45° to the beam path (Fig. 1).

Assuming ~4% reflection at air/glass interfaces, ~8% of the laser light was directed towards the photodiode in this setup. The photodiode was connected to an oscilloscope.

Our initial observations revealed an absence of mode locking in the laser: laser light was not emitted in regular pulses. Mode locking was achieved with the help of a Clark-MXR technical representative, by adjusting the wave plates.

Figures

Figure Legends

FIG. A1. Schematic of second harmonic generation. (<http://moebius.physic.tu-berlin.de>)

FIG. 1. One configuration of the optical apparatus.

FIG. 2. Fluorescence emission spectra for various dyes.

A. DiI (<http://probes.invitrogen.com/servlets/spectra?fileid=282lip>).

B. di-4-ANEPPS. Spectra measured in a formalin-fixed rabbit heart with 2-photon excitation at 930 nm (solid) and single-photon excitation at 488 nm (dotted) (Dumas and Kinsley 2005).

C. di-8-ANEPPS (<http://probes.invitrogen.com/servlets/spectra?fileid=3167lip>).

D. Rhodamine 6G
(<http://omlc.ogi.edu/spectra/PhotochemCAD/html/rhodamine6G.html>).

E. Rhodamine B (<http://omlc.ogi.edu/spectra/PhotochemCAD/html/rhodamineB.html>).

FIG. A1

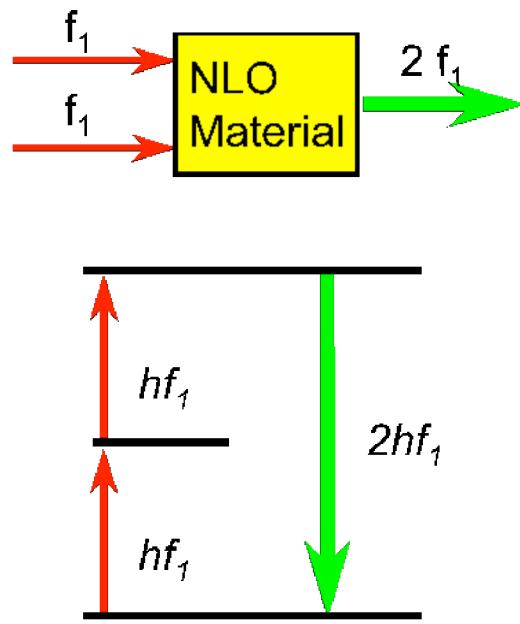


FIG. 1

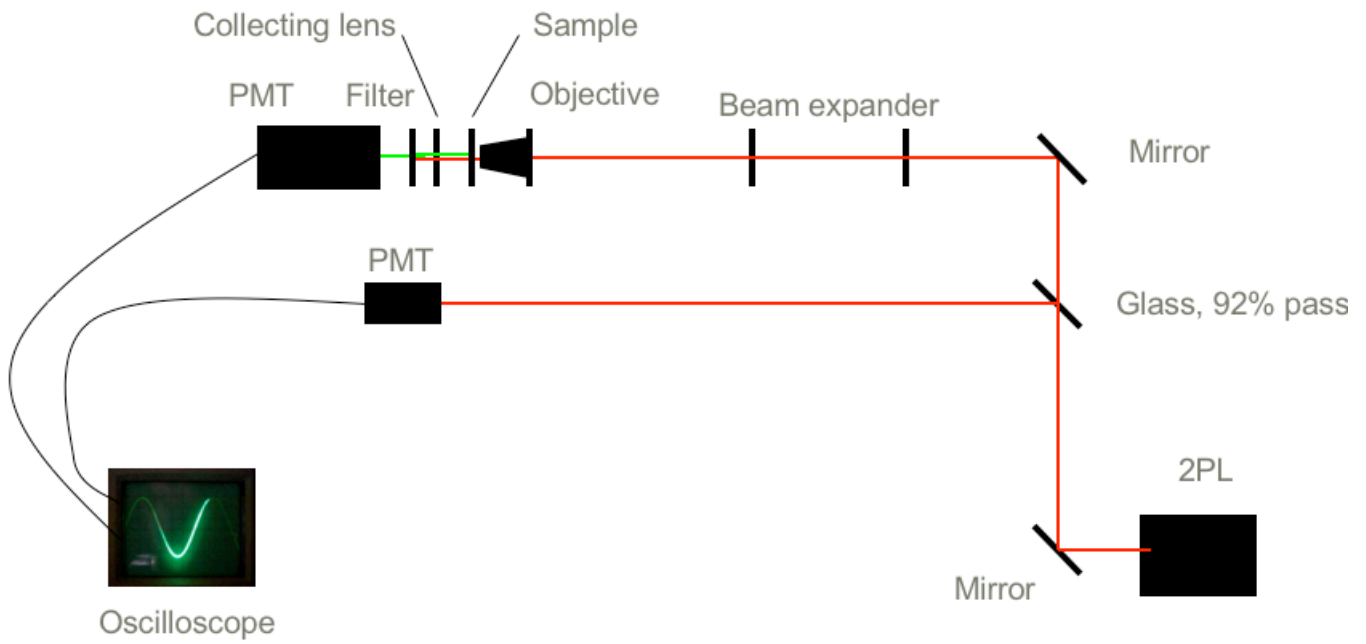
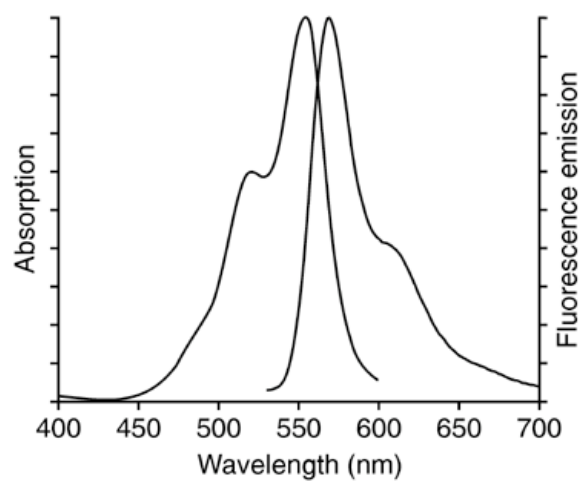
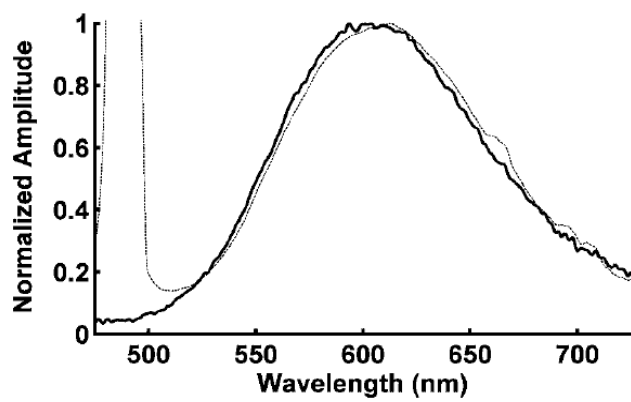


FIG. 2

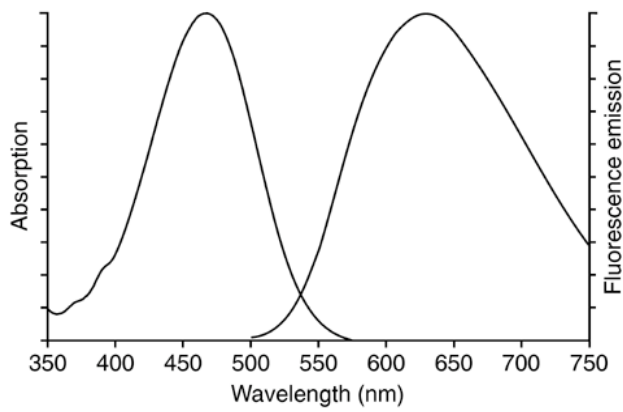
A



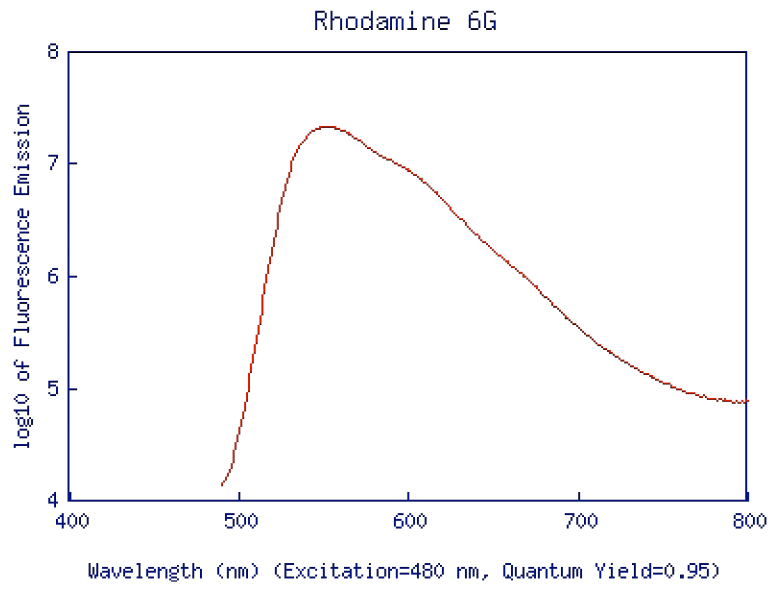
B



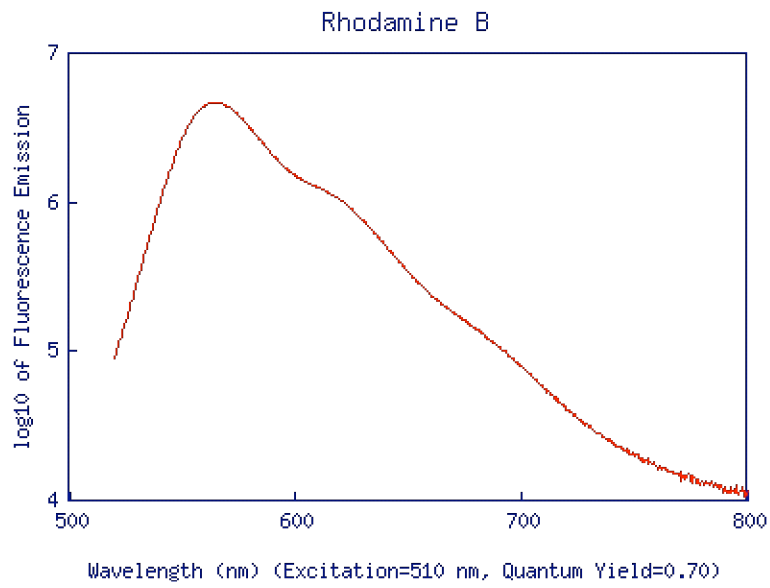
C



D



E



References

[Brzezinski P, Messinger A, Blatt Y, Gopher A, Kleinfeld D](#). Charge displacements in interfacial layers containing reaction centers. *J Membr Biol*. 1998 Oct 1;165(3):213-25.

[Both M, Vogel M, Friedrich O, von Wegner F, Kunsting T, Fink RH, Uttenweiler D](#). Second harmonic imaging of intrinsic signals in muscle fibers in situ. *J Biomed Opt*. 2004 Sep-Oct;9(5):882-92.

[Bouevitch O, Lewis A, Pinevsky I, Wuskell JP, Loew LM](#). Probing membrane potential with nonlinear optics. *Biophys J*. 1993 Aug;65(2):672-9.

Boyd, RW. *Nonlinear Optics*. San Diego: Academic Press (1992).

[Brian AA, McConnell HM](#). Allogeneic stimulation of cytotoxic T cells by supported planar membranes. *Proc Natl Acad Sci U S A*. 1984 Oct;81(19):6159-63.

[Brown RM Jr, Millard AC, Campagnola PJ](#). Macromolecular structure of cellulose studied by second-harmonic generation imaging microscopy. *Opt Lett*. 2003 Nov 15;28(22):2207-9.

[Campagnola PJ, Millard AC, Terasaki M, Hoppe PE, Malone CJ, Mohler WA](#). Three-dimensional high-resolution second-harmonic generation imaging of endogenous structural proteins in biological tissues. *Biophys J*. 2002 Jan;82(1 Pt 1):493-508.

Cremer PS, Boxer SG. Formation and Spreading of Lipid Bilayers on Planar Glass Supports. *J. Phys. Chem. B* 1999 103:2554-2559.

Denk W, Strickler JH, Webb WW, *Science*, **248**, 4951, 73-76, (1990).

[Dumas JH 3rd, Knisley SB](#). Two-photon excitation of di-4-ANEPPS for optical recording of action potentials in rabbit heart. *Ann Biomed Eng*. 2005 Dec;33(12):1802-7.

Franken PA, Hill AE, Peters CW, and Weinreich G, *Phys. Rev. Lett.* **7**, 118 (1961).

Friedrich DM, Two-photon molecular spectroscopy. *J. Chem. Educ* **59** (1982), pp. 472-481.

Goeppert-Mayer M, *Ueber Elementarakte mit zwei Quantenspruengen*. *Ann. Phys* **9** (1931), p. 273.

Hecht, E. *Optics (4e)*. Reading, MA: Addison-Wesley (2002).

[Lichtenberg D, Romero G, Menashe M, Biltonen RL](#). Hydrolysis of dipalmitoylphosphatidylcholine large unilamellar vesicles by porcine pancreatic phospholipase A2. *J Biol Chem*. 1986 Apr 25;261(12):5334-40.

[Millard AC, Jin L, Lewis A, Loew LM](#). Direct measurement of the voltage sensitivity of second-harmonic generation from a membrane dye in patch-clamped cells. *Opt Lett*. 2003 Jul 15;28(14):1221-3.

[Millard AC, Jin L, Wuskell JP, Boudreau DM, Lewis A, Loew LM](#). Wavelength- and time-dependence of potentiometric non-linear optical signals from styryl dyes. *J Membr Biol*. 2005 Nov;208(2):103-11.

[Moreaux L, Sandre O, Charpak S, Blanchard-Desce M, Mertz J](#). Coherent scattering in multi-harmonic light microscopy. *Biophys J*. 2001 Mar;80(3):1568-74.

[Nemet BA, Nikolenko V, Yuste R](#). Second harmonic imaging of membrane potential of neurons with retinal. *J Biomed Opt*. 2004 Sep-Oct;9(5):873-81.

[Nuriya M, Jiang J, Nemet B, Eisenthal KB, Yuste R](#). Imaging membrane potential in dendritic spines. *Proc Natl Acad Sci U S A*. 2006 Jan 17;103(3):786-90. Epub 2006 Jan 9.

[Sacconi L, Dombeck DA, Webb WW](#). Overcoming photodamage in second-harmonic generation microscopy: real-time optical recording of neuronal action potentials. *Proc Natl Acad Sci U S A*. 2006 Feb 28;103(9):3124-9. Epub 2006 Feb 17.

[Sackmann E](#). Supported membranes: scientific and practical applications. *Science*. 1996 Jan 5;271(5245):43-8.

[Sandre O, Moreaux L, Brochard-Wyart F](#). Dynamics of transient pores in stretched vesicles. *Proc Natl Acad Sci U S A*. 1999 Sep 14;96(19):10591-6.

[Schonherr H, Johnson JM, Lenz P, Frank CW, Boxer SG](#). Vesicle adsorption and lipid bilayer formation on glass studied by atomic force microscopy. *Langmuir*. 2004 Dec 21;20(26):11600-6.

[Stottrup BL, Veatch SL, Keller SL](#). Nonequilibrium behavior in supported lipid membranes containing cholesterol. *Biophys J*. 2004 May;86(5):2942-50.

Tsai PS, Nishimura N, Yoder EJ, Dolnick EM, White GA, et al. Principles, design, and construction of a two photon laser scanning microscope for in vitro and in vivo brain imaging. In: Frostig RD, editor *In vivo optical imaging of brain function*. Boca Raton (Florida): CRC Press. 113–171 (2002).

Webb WW and Svoboda K. Photon Upmanship: Why multiphoton imaging is more than a gimmick. *Neuron*, **18** (3), 351-357 (1997).

[White G, Pencer J, Nickel BG, Wood JM, Hallett FR](#). Optical changes in unilamellar vesicles experiencing osmotic stress. *Biophys J*. 1996 Nov;71(5):2701-15.

[Williams RM, Zipfel WR, Webb WW](#). Interpreting second-harmonic generation images of collagen I fibrils. *Biophys J*. 2005 Feb;88(2):1377-86. Epub 2004 Nov 8

[Wong M, Anthony FH, Tillack TW, Thompson TE](#). Fusion of dipalmitoylphosphatidylcholine vesicles at 4 degrees C. *Biochemistry*. 1982 Aug 17;21(17):4126-32.